# Impact of Multipath Interference on the Performance of an UWB Fast Acquisition System for Ranging in an Indoor Wireless Channel

Yassine SALIH ALJ[1,2], *Student Member, IEEE,* Charles DESPINS[1,2,3], *Senior Member, IEEE,* and Sofiène AFFES[1,2], *Senior Member, IEEE*

1: INRS-E.M. & Telecommunications, 800, De La Gauchetière West, Suite 6900, Montreal (QC) H5A 1K6 Canada.
2: Underground Communications Research Laboratory (LRCS), 450, 3d Av., Local 103, Val-d'Or (QC) J9P 1S2 Canada.
3: Prompt, 1155, University Street, Suite 903, Montreal (Qc) H3B 3A7 Canada.
Email: yassine@emt.inrs.ca; cdespins@promptinc.org; affes@emt.inrs.ca
Tel.: +1.514.875.1266 ext.2011

## Abstract

*In this paper, the effects of multipath interferences on the performance of a multiuser ultra-wideband (UWB) fast acquisition system operating in an underground indoor fading channel are evaluated and compared. Various pulse shapes are considered with different scenarios of interference and Gaussian noise in extensive Monte-Carlo simulations. The results show the 6th order Gaussian derivative as the most suitable pulse shape for this new UWB fast acquisition system suggested for ranging in a peculiar confined environment, offering very acceptable positioning error range at high levels of noise and interference, while also yielding greatly reduced complexity and acquisition time.*

## I. Introduction

Ultra-wideband (UWB) technology is currently regarded as an attractive solution for many wireless applications where high resolution, reduced interference, and propagation around obstacles are challenging [1]. It utilizes ultra-short pulse shapes transmitted at a very low Power Spectral Density (PSD) in compliance to the Federal Communications Commission (FCC) rules that defined UWB signal with a fractional bandwidth greater than or equal to 0.2 of the center frequency or a bandwidth of at least 500 MHz [2].

Timing acquisition is known as one of the key technical aspects that influence the successful development of UWB systems. In fact, the extremely narrow time frames and implicitly the required high sampling rates make signal acquisition and the overall UWB transceiver design/operation a challenging task from a technical viewpoint [3]. In recent years, much research work has been devoted to accelerating the acquisition process of UWB signals. Based on different algorithmic approaches, several fast acquisition techniques were proposed [4-7]. However, the complexity aspect was generally less emphasized than the algorithmic one. Indeed, the correlations are computed in the time domain and acquisition systems are fed by stream processing, sample by sample, irrespective of the search strategy (serial or parallel) [3]. The corresponding architectures are thus not optimal and may require relatively long processing times under challenging conditions, e.g. inside an underground mine gallery. Few studies available in the literature today consider this peculiar environment [8-9]. However, UWB technology, as a physical support with excellent temporal resolution, is very promising in this area [10]. In order to achieve a low-complexity receiver, an UWB computationally-efficient acquisition system showing explicit design characteristics that offer greatly improved computational cost and acquisition time was proposed in [11].

In this paper, we evaluate the performance of this new UWB fast acquisition system suggested for ranging within a peculiar multipath fading channel. The suggested scheme, based on a *block-processing* technique adapted to a *high-speed* frequency correlator by a *cubic spline interpolation*, is validated by performance comparisons under different scenarios of interference and Gaussian noise. Furthermore, in addition to the PSD of the transmitted signal which is influenced by the used pulse shape, the performance of the UWB system itself may also be affected under non-ideal conditions [12]. Thus, the choice of the fundamental pulse shape to adopt within the system is one of the most important considerations that may affect its performance. In [13], the first ten Gaussian derivatives were compared in terms of their PSD and compliance to the FCC spectral constraints. For these pulses, higher-order derivatives have shown a better fit to the FCC masks with a decreasing bandwidth as the order of the derivative increases. Moreover, Gaussian-based pulse shapes outperform generally other UWB typical pulse types, as recently proposed in [14], and are noticeably easier to generate [15]. These observations lead to considering Gaussian-based waveforms, typically high-order derivatives, as the most potential candidates for the suggested UWB system.

The remainder of this paper is organized as follows. In Section II, the system model is given. Section III details the proposed UWB fast acquisition system. Simulation results are provided in Section IV, and Section V concludes the paper.

## II. System Model

In this section, we will describe the system model of the considered UWB communication system.

978-0-7695-3135-9/08 $25.00 © 2008 IEEE
DOI 10.1109/CNSR.2008.17

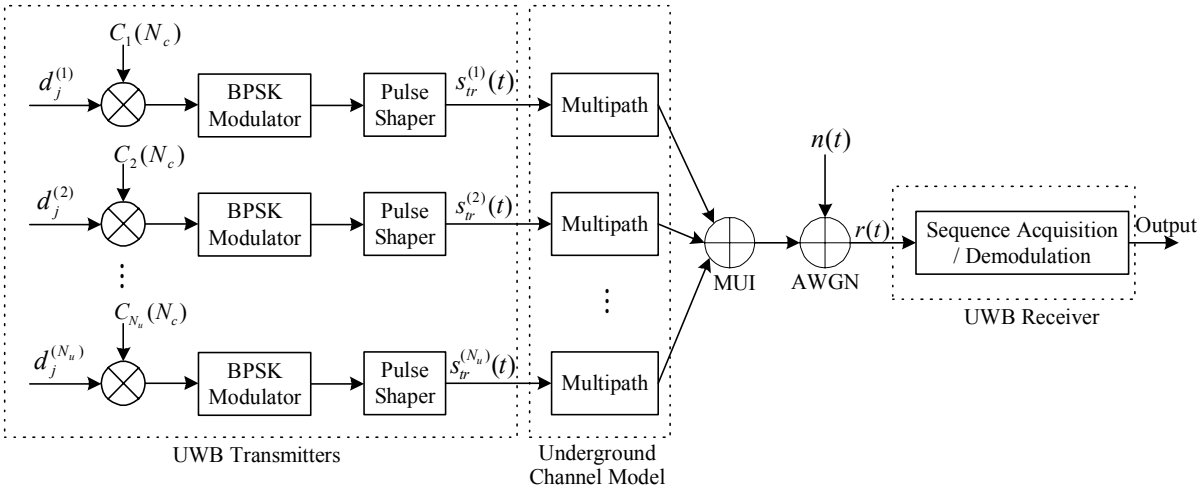


Fig.1. Block diagram of the considered system model

### A. *UWB Transmitter*

Direct-Sequence (DS) UWB concept is employed in this paper with BPSK pulse signaling. The pulse occupies the entire chip interval and is transmitted continuously according to a MLS spreading code. The DS-UWB signal transmitted by a user $k$ can typically be expressed as

$$s_{tr}^{(k)}(t) = \sum_{j=-\infty}^{j=+\infty} \sum_{n=0}^{N_c-1} d_j^{(k)} \cdot c_n^{(k)} \cdot p_{tr}(t - jT_f - nT_c), \qquad (1)$$

where $p_{tr}(t)$ represents the transmitted pulse shape (*i.e.* Gaussian 5$^{th}$-order derivative), $\{d_j\}$ represent the modulated data symbols mapped into {-1, 1}, $\{c_n\}$ are the spreading chips generated according to a MLS code, $T_c$ is the chip duration. There are $N_c$ chips per each message symbol $j$ of period $T_f$ − the spreading factor − such that $N_c . T_c = T_f$.

### B. *Pulse Shape*

The transmitted pulse shape used within an UWB system influences its spectral properties. The considered ultra-short pulse duration $T_c$ is 2 ns, so the effective UWB signal bandwidth is at least 500 MHz. Moreover, due to antenna effects, the processed pulse at the receiver is modeled as a derivative of the transmitted pulse shape. The basic Gaussian pulse is expressed as

$$p(t) = \frac{1}{\sqrt{2\pi}\sigma} \exp\left(-\frac{t^2}{2\sigma^2}\right), \qquad (2)$$

where σ is a shape factor used typically as a bandwidth decaying parameter. The n$^{th}$ order Gaussian derivative can be determined recursively from

$$p_n(t) = -\frac{n-1}{\sigma^2} p_{n-2}(t) - \frac{t}{\sigma^2} p_{n-1}(t) \cdot \qquad (3)$$

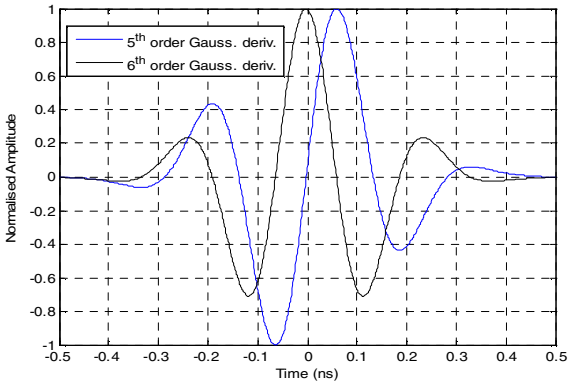


Fig. 2. 5$^{th}$ and 6$^{th}$ order Gaussian derivatives pulse shapes in time domain.

The amplitude spectrum of the n$^{th}$ order Gaussian derivative, obtained from its Fourier transform, is

$$|X_n(f)| = (2\pi f)^n \exp\left\{-\frac{(2\pi f\sigma)^2}{2}\right\}. \qquad (4)$$

By differentiating (4) and setting it equal to zero, the peak transmission frequency $f_p$, at which the maximum is attained, can be found to satisfy the following:

$$2\pi f_p \sigma = \sqrt{n} \cdot \qquad (5)$$

Then, the Gaussian derivatives of higher orders are characterized by a higher peak frequency while reducing the shape factor σ shortens the pulse. Notice that the PSD of the first order Gaussian derivative does not meet the FCC requirement no matter what value of pulse width is used. Moreover, increasing the order of the derivative results in a wider overall pulse width for each successive pulse and, consequently, in a narrower bandwidth around the same center frequency, thereby showing a better fit to the FCC masks. Indeed, as the pulse order increases, the number of zero crossings in the same pulse width also increases. The pulses then begin to resemble sinusoids modulated by a Gaussian pulse-shaped envelope, thus corresponding to a higher "carrier" frequency sinusoid modulated by an equivalent Gaussian envelope [12].

### C. *Underground UWB Channel Model*

The considered discrete impulse response of the UWB channel model for underground mine is expressed as the following:

$$h(t) = \sum_{l=0}^{L-1} \alpha_l \delta(t - \psi_l), \qquad (6)$$

where $\delta(t)$ is the Dirac delta function, $L$ is the number of multipath components; $\{\alpha_l\}$ and $\{\psi_l\}$ are, respectively, the gain and the delay introduced by the $l^{th}$ path of the channel. Note that a complex tap model is not adopted here. The complex baseband model is a natural fit for narrowband systems to capture channel behavior independently of carrier frequency, but this motivation breaks down for UWB systems where a real-valued simulation at RF may be more natural [16]. As for the IEEE.802.15.3a standard model, lognormal distribution has been used for the multipath gain. For the data measurements obtained in the considered mining environment, this chosen distribution was confirmed by the Kolmogorov-Smirnov test [17].

Furthermore, as in the Saleh-Valenzuela model the first ray starts by definition at $t$=0, and the successive rays arrive with a rate given by a Poisson process with rate $\lambda$=1.15 $(ns)^{-1}$ (*i.e.* of 2.3 rays per chip). The power of these rays decays exponentially with increasing delay from the first ray. However, for the considered mining environment in contrast to what was reported for more conventional indoor environments with smooth surfaces [16] [18], no path clustering effect was observed, neither in NB/WB measurements [9], nor in the LOS scenario at recent UWB measurements work done in such confined environments with rough surfaces [17]. Indeed, since this work is intended for a ranging application, we focus only on the LOS scenario where the first path is assumed the direct and strongest from what the Time-of-Flight TOF is estimated. Figs. 3 and 4 show, respectively, a typical underground impulse response obtained by channel sounding and its corresponding lognormal PDF.

A threshold of 40 dB below the strongest path was chosen to avoid the effect of noise on the statistics of multipath channel [17]. Hence in the interest of simplicity, we consider the impulse response restricted to $L$=3 paths (*i.e.* two interfering paths to the direct first path). As for our ranging application we focus on the direct path (*i.e.* strongest), its gain is normalized to unity. However, we take into account SNR as the ratio of the total power of all paths and the noise level. The lognormal fading statistics of the two interfering paths are as expressed in Table I. Their relative variance is, as it seems intuitively clear, smaller for small gain than for large one, a fact that was confirmed, e.g. in [19].

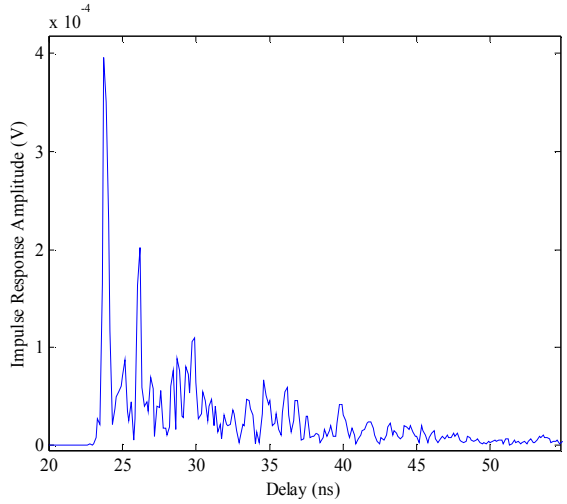


Fig. 3. Typical underground impulse response in LOS scenario.

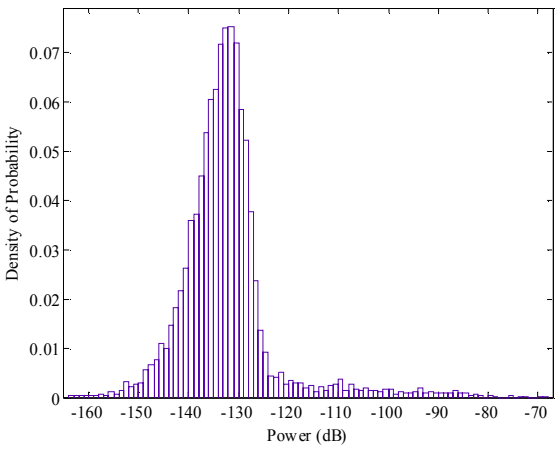


Fig. 4. Probability Density Function of the received signal in LOS scenario.

TABLE I. LOGNORMAL FADING PARAMETERS

| Interfering Paths | Lognormal Statistics | |
|---|---|---|
| | $E[\alpha_l]$ | $Var[\alpha_l]$ |
| $l$=1 | 0.5 | 0.09 |
| $l$=2 | 0.25 | 0.04 |

### D. UWB Receiver

When $N_u$ users are active within the system, while focusing on a transmitter $k$, the signal at the receiver can be modeled as

$$r(t) = \sum_{l=0}^{2} c_l s_{pr}^{(1)}(t-\theta_l) + n_g(t), \quad (7)$$

where $c_l$ the is the amplitude fading factor on the $l^{th}$ path, $\theta_l$ is a summation of the delay $\psi_l$ exclusively introduced by the $l^{th}$ path and the phase-shift $\tau^{(k)}$ that corresponds to the TOF between the transmitter $k$ and the considered receiver. $\theta_l$ is exponentially distributed ($\mu$=0.87), the fading factor $c_l$ of the interfering paths is lognormally distributed as

$$20\log_{10}(c_1) \propto N(-0.8469,\ 0.3075), \quad (8)$$

$$20\log_{10}(c_2) \propto N(-1.6336,\ 0.4947), \quad (9)$$

based on the values expressed in Table I, and $n_g(t)$ is

$$n_g(t) = \sum_{k=2}^{N_u} \sum_{l=0}^{2} s_{pr}^{(k)}(t-\theta_l) + n(t), \quad (10)$$

in which $s_{pr}(t)$ corresponds to $p_{pr}(t)$, the processed pulse shape at the receiver (antenna effect). $n(t)$ represents the received Gaussian noise modeled as $N(0,\ \sigma_n^2)$ with a power spectral density of $N_0/2$.

## III. DS-UWB FAST ACQUISITION SYSTEM

### A. Processing Technique

The *Block-Processing* technique was used with an *FFT-based high-speed* frequency correlator that offered a fast and accurate acquisition of the dense DS-UWB signal with optimal receiver complexity. This method suggested for UWB signal acquisition is valuable in view of its efficiency in real time handling of high data throughputs [20] and has shown high effectiveness in other fields [21-22]. The acquisition process is accelerated by handling the dense UWB signal in simultaneous blocks of samples and by reducing efficiently the computational cost. The samples of the acquired UWB signal are stored in blocks as they arrive. The processing of a block starts when its last sample arrives and proceeds simultaneously with the storage of the next block. Block-Processing techniques can be used when the input sample rate is much greater than the output sample rate [20]. For a DS-UWB receiver, processing is performed on each acquired block $i$ to evaluate a code phase-shift $\tau_i$ and a Signal to Interference plus Noise Ratio $SINR_i$. Since the block must cover at least a whole spreading code period (*i.e.* several hundred samples), and the output is only two values per block, the conditions for block processing are satisfied.

Synchronization is performed by an FFT-based circular correlator fed by the handled blocks. The block length $M$ is taken as of power-of-two; thus the used FFTs have an optimal butterfly structure. Hence, the correlation is computed in the frequency domain by a simple multiplication, producing the same result as the standard correlation but faster with this high-speed correlation technique. The fast correlator structure can be further optimized by avoiding the FFT used for the local replica which can be pre-calculated. Therefore, the correlator will require only one FFT/IFFT pair. The processed DS-UWB received signal can be modeled as

$$r_{i,u}^{(j,N_u)} = d_{u,\tau_i}^{(j,k)} c_{i,\tau_i}^{(j,k)} p_{pr}\left((m_i+u) - jT_f - \frac{N_c}{M}(m_i+u)\,T_c - \tau_i^{(k)}\right) + n_{f_{(i,u)}} + n_{g_{(i,u)}}^{N_u}, \quad (11)$$

where $p_{pr}()$ represents the processed pulse shape at the receiver (antenna derivative effect), $n_f$ is the interference signal, $u$ refers to the $u^{th}$ sample ($u$=1, 2, ..., $M$) of the $i^{th}$ block, $m_i$ is the total number of samples before the $i^{th}$ block ($m_i$=(i-1).$M$) and $k$ corresponds to the acquired user at the receiver.

Since the received signal $r_{i,u}$ and the local pulse-shaped replica corresponding to the acquired MLS spreading code $c_{i,\tau_i}$ are both finite length sequences, their correlation can be carried out by a slight modification of the circular convolution operation. Indeed, the correlation of these two sequences is obtained by tacking the product of their discrete Fourier transforms DFTs while the local pulse-shaped replica is time reversed, thus a complex conjugate is applied. Therefore, the resulting correlation performed in the frequency domain, $R_{i,u}$, of the $i^{th}$ received signal block, $r_{i,u}$, with the local pulse-shaped replica of the $k^{th}$ user, can be expressed as the following:

$$R_{i,u}^{(k)} = IDFT\left\{ DFT\left\{ r_{i,u}^{(N_u)} \right\} \cdot DFT^{*}\left\{ c_i^{(k)} p_{pr}[(m_i+u)\cdot(1-N_c T_c/M)] \right\} \right\}. \quad (12)$$

In practice, the FFT is used as an efficient algorithm, to calculate the DFTs required in this frequency-domain correlation operation.

### B. UWB Acquisition Scheme

The block diagram of the proposed UWB fast acquisition system is shown in Fig. 5. Its significant parameters include: a spreading factor $N_c$= 63; a pulse duration $T_p$= $T_c$= 2 ns (a duty cycle of 100 %); number of samples per chip $N_s$=16 (sampling frequency $F_s$= $N_s/T_c$= 8 GHz); a Gaussian 6th-order derivative as the acquired pulse waveform; and an increased block length $M=(1+N_c).N_s$=1024. Notice that recent developments in research institutions and industry promise high sampling rates with great resolutions for both ADCs and FFTs [23-24].

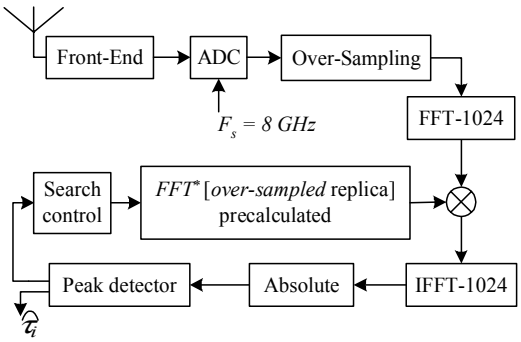


Fig. 5. Block diagram of the UWB fast acquisition system.

An *over-sampling* method is required for adapting efficiently as possible the acquired block's length to the FFTs of butterfly structure. Thus, the cardinality of the blocks digitized by the ADC converter should be increased from 1008 samples to 1024 (a power-of-two). Then the correlation is calculated in the frequency domain by a fast circular correlator. A peak detector examines its outputs (1024 inverse-FFT outputs) to evaluate the detected peak amplitude and to deduct its position which corresponds to the estimated phase-shift $\tau_i$. The more blocks are acquired; the more refined will be that estimated phase which represents the TOF required for ranging with respect to the acquired user. If no peak is detected according to a detection threshold $D_T$, the search control block leads the local code generator index to the next pre-calculated replica *k+1*. To locate itself, the claimant (*i.e.* receiver) can use 2D-trilateration with respect to two *verifiers* (*i.e.* static transmitters).

In order to characterize the relative amplitude of the detected peak with respect to false correlations due to interferences and noise, an acquisition margin is considered. Since the direct path amplitude is normalized to unity, while the noise level is set bellow 18 %, an acquisition margin of 14.9 dB is used for the detection.

### C. Gain in Complexity

Assuming that a multiplication computation takes as much as two addition operations, then the total required operations by this UWB acquisition scheme is $6\log_2 M+2M$. Thus, the gain in complexity of this studied fast DS-UWB acquisition system (in comparison to a traditional system[1]) can be modeled in terms of the used spreading factor as

$$G = 1.5\cdot 10^{-6}\cdot N_c^{\,3} - 9.2\cdot 10^{-4}\cdot N_c^{\,2} + 0.77\cdot N_c + 2.6\,. \quad (13)$$

We note for a spreading factor of 63, a significant reduction in the computational cost by a factor of about 48. Consequently, the acquisition time is considerably improved with a computational cost reduction.

## IV. Simulation Results

In this section, the performance of the studied UWB multiple-access fast acquisition system in the considered underground channel model are evaluated, by extensive Monte-Carlo simulations, using 100 000 samples. The performance are assessed in terms of the obtained positioning error range which corresponds to the synchronization error obtained while estimating the phase-shift $\tau$. Four different acquisition systems are compared, including ours to validate its score in comparison to the other systems. Furthermore, the performance of the first eleven Gaussian derivatives and the doublet waveforms are compared while used within the studied UWB fast acquisition system to determine the most suitable pulse shape to consider in the multipath scenario for that proposed scheme. Moreover, the obtained performance of the studied computationally-efficient system is compared with respect to the unipath case under different levels of MUI and AWGN. The PN sequences of the interfering sources are randomly selected from $N_{umax}$=6 MLS codes of period $N_c$=63. Moreover, as a considered worst case of MUI constraint, the interfering users are supposed synchronous with the receiver.

Fig. 6 illustrates the performance comparison of the standard acquisition system based on time-domain correlation and the fast acquisition system simulated without an over-sampling method (non-optimal FFT of 1008 points), with *zero-padding*, and finally with the suggested *cubic spline interpolation*. We notice notable performance degradation for the fast acquisition system based on zero-padding. Indeed, this technique changes the circular correlation properties. This is due to the fact that the insertion of the zero divides the MLS code into two subsequences. Thus, the resulting autocorrelation function contains two neighboring peaks instead of one. Thus, the obtained positioning error range fluctuates, as noticed, slightly with respect to the strongest peak detected between the two neighboring peaks in the resulting autocorrelation function. This observed energy loss affects the estimation accuracy and the overall detection capabilities, thus increasing the probability of misdetection. However, we note from the comparisons that the suggested computationally-efficient fast acquisition

[1] It requires $M^2$ multiplications and $M^2$-*1* addition operations.

system, *based on interpolation as an over-sampling method*, maintains in the considered multipath scenario very acceptable levels of accuracy in terms of location estimation, while offering an improved acquisition time with a greatly reduced complexity.

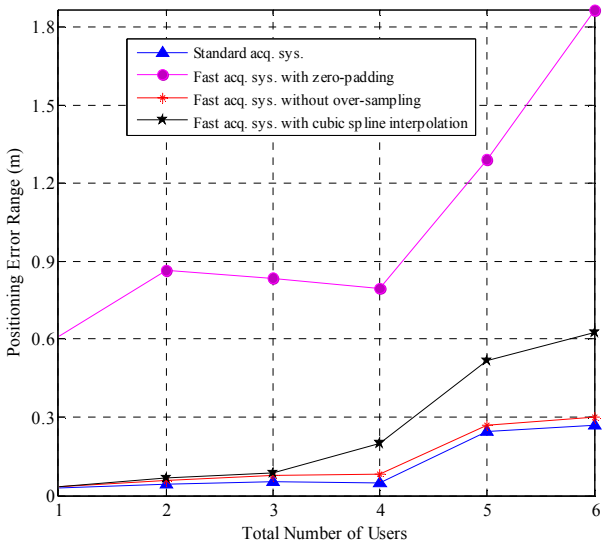


Fig. 6. Performance comparison in multipath channel under MUI and AWGN ($\sigma_N^2$=0.5).

As noticed, the cubic spline interpolation used as an over-sampling technique changes the overall correlation properties of the pulse shapes. Hence, these will behave herein differently in comparison to other standard acquisition systems. The considered Gaussian-based pulse shapes were run under MUI in extensive Monte-Carlo simulations and compared in the considered multipath context while the noise variance was taken $\sigma_n^2$=2. Fig. 7 shows the performance degradation of the simulated waveforms within the proposed fast acquisition system. We notice that the best performance score is obtained by the 10$^{th}$ Gaussian derivative and a bit lower level by, the 8$^{th}$ Gaussian derivative and then the 6$^{th}$-order derivative. These waveforms are the most suitable pulse shapes to choose, depending on the spectral bandwidth requirements, since the 6$^{th}$ derivative offers a wider bandwidth. Indeed, as the derivative order increases, the peak transmission frequency increases and the signal bandwidth decreases. Hence, choosing the most appropriate derivative order is a trade-off with the pulse shape factor for a desired performance level. Therefore, tacking into account bandwidth maximization as an important design factor, the 6$^{th}$ order Gaussian derivative has been validated for this studied UWB fast acquisition system in the considered indoor fading channel.

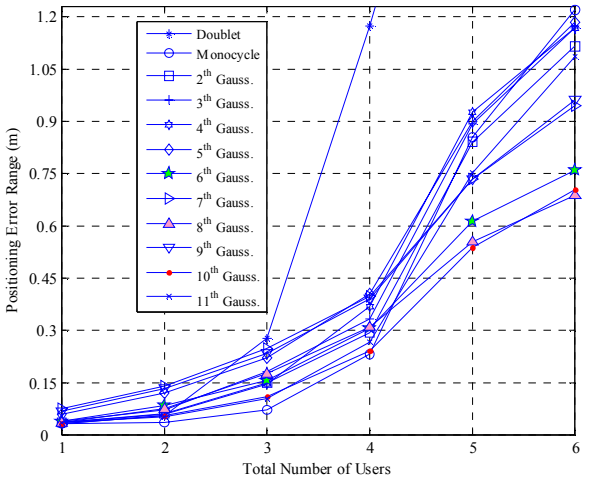


Fig. 7. Pulse shapes performance comparison in multipath scenario under MUI and AWGN ($\sigma_N^2$=2).

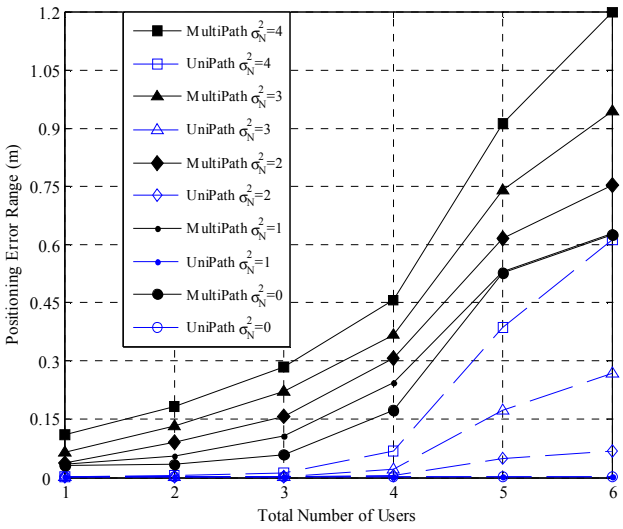


Fig. 8. Performance comparison between multipath and unipath scenarios under MUI and AWGN levels.

Fig. 8 shows the performance levels for both scenarios of multipath and unipath, compared under MUI and AWGN levels. From these results, we note a maximum gap of 0.6 meters in the positioning error range between the multipath and unipath scenarios. However, since we obtain for the worst case (*i.e.* maximum interfering sources within the system with a high level of noise; $\sigma_N^2$=4) a location estimation precision of 1.2 meters which is very acceptable for the desired ranging application, we consider the suggested fast acquisition system well-suited for such underground confined environment.

## V. CONCLUSION

In this paper, an UWB fast acquisition system has been proposed for ranging in a peculiar indoor multipath fading channel. The performance of the suggested computationally-efficient fast acquisition system were assessed and compared in an underground mining environment. Simulation results have shown that the proposed fast acquisition scheme based on interpolation offers greatly reduced complexity and acquisition time, while also yielding very satisfactory performance at high levels of MUI and AWGN. Furthermore, different Gaussian-based pulses were compared in extensive Monte-Carlo simulations to evaluate their effect on the performance of the suggested system. The results have validated the $6^{th}$-order Gaussian derivative as the most suitable pulse shape to adopt for this system operating in such considered confined environment. Moreover, comparisons of the suggested fast acquisition system have been made between the considered multipath fading channel and a unipath scenario, with respect to the obtained location estimation precision. The proposed system has shown very acceptable positioning error range for the considered mining environment.

## REFERENCES


[1] A. Dogandzic, J. Riba, G. Seco and A.L. Swindlehurst, "Positioning and navigation with applications to communications," in *IEEE Signal Proc. Magazine*, Vol. 22, No. 4, pp. 10–11, Jul. 2005.

[2] Federal Communications Commission "Revision of part 15 of the commission's rules regarding ultra-wideband transmission systems," First Report and Order, ET Docket 98–153, April 2002.

[3] L Reggiani and G.M. Maggio, "On the acquisition time for serial and parallel code search in UWB impulse radio," in *Proc. IEEE Int. Symp. on Circuits & Systems ISCAS'05*, Vol. 1, pp.53 – 56, May 2005.

[4] S.R. Aedudodla, S.Vijayakumaran and T.F.Wong, "Timing acquisition in ultra-wideband communication systems," in *IEEE Trans. on Vehicular Technology*, Vol. 54, No. 5, pp.1570-1583, Sept.2005.

[5] L. Reggiani and G. M. Maggio, "Rapid search algorithms for code acquisition in UWB impulse radio communications," in *IEEE Journal on Selected Areas in Comm.*, Vol. 23, No. 5, pp. 898-908, May 2005.

[6] W. Namgoong, "A Channelized Digital Ultra-Wideband Receiver," in *IEEE Trans. Wireless Comm.*, Vol. 2, pp. 502-510, May 2003.

[7] N. He and C. Tepedelenlioglu, "Fast and Low-Complexity Frame-Level Synchronization for Transmitted Reference Receivers," in *IEEE Trans. on Wireless Comm.*, Vol. 6 , No. 3, pp. 1014 – 1023, March 2007.

[8] C. Nerguizian, C. Despins, S. Affes and M. Djadel, "Radio channel characterization of an underground mine at 2.4 GHz," in *IEEE Trans. on Wireless Comm.*, Vol. 4, No. 5, pp. 2441–2453, Sept. 2005.

[9] M. Boutin, A. Benzakour, C. Despins and S. Affes, "Radio Wave Characterization and Modeling in Underground Mine Tunnels," *in IEEE Trans. on Antennas and Propagation*, August 2007, in press.

[10] C. Nerguizian, "Radiolocation in an underground mining environment," Ph.D. dissertation, INRS-EMT, Montreal, Canada, Sept. 2003.

[11] Y. Salih Alj, C. Despins, and S. Affes, "A computationally efficient implementation of a UWB fast acquisition scheme," in *Proc. IEEE VTC'07-Spring*, pp. 1554-1558, April 2007.

[12] M. Welborn and J. McCorkle, "The importance of fractional bandwidth in ultra-wideband pulse design," in *Proc. IEEE Int. Conf. Communications*, Vol. 2, pp. 753–757, April 2002.

[13] H. Sheng, P. Orlik, A.M. Haimovich, L.J. Cimini, and J. Zhang, "On the spectral and power requirements for ultra-wideband transmission," in *Proc. IEEE Int. Conf. Communications*, Vol. 1, pp.738–742, May 2003.

[14] B. Hu and N.C. Beaulieu, "Pulse shapes for ultrawideband communication systems," in *IEEE Trans. on Wireless Communications*, Vol. 4, No. 4, pp. 1789–1797, July 2005.

[15] M.U. Mahfuz, K.M. Ahmed, R. Ghimire and R.M.A.P. Rajatheva, "Performance comparison of pulse shapes in STDL and IEEE 802.15.3a models of the UWB channel," in *Proc. IEEE ICICS'05*, pp.811–815, Dec. 2005.

[16] J. R. Foerster, M. Pendergrass and A. F. Molisch, "A channel model for ultrawideband indoor communication," in *Wireless Personal Multimedia Communications WPMC'03*, Vol. 2, pp. 116–120, October 2003.

[17] Y. Rissafi, "Characterization and modeling of ulta-wideband channel in an underground mine," Masters's thesis, University of Quebec at Outaouais, Canada, June 2007.

[18] A.A. Saleh, R. A. Valenzuela, "A statistical model for indoor multipath propagation," in *IEEE Journal on Selected Areas in Communications*, Vol. 5, No. 2, pp. 128–137, Feb. 1987.

[19] D. Cassioli, Moe Z. Win and Andreas F. Molisch, "The ultra-wide bandwidth indoor channel: from statistical model to simulations", in *IEEE Journal on Selected Areas in Communications*, Vol. 20, No. 6, pp. 1247–1257, August 2002.

[20] J.G. Ackenhusen, Real-time signal processing: design and implementation of signal processing systems, Prentice Hall, 1999.

[21] P.M. Gerard, G.P.M. Egelmeers and P.C.W. Sommen, "A new method for efficient convolution in frequency domain by nonuniform partitioning for adaptive filtering," in *IEEE Trans. on Signal Proc*, Vol. 44, No. 12, pp.3123 – 3129, Dec. 1996.

[22] G. Feng and F. Van Graas, "GPS receiver block processing," in Proc. ION Institute Of Navigation GPS-99, pp. 307– 316, Sep. 1999.

[23] O. A. Mukhanov et al., "High-resolution ADC operation up to 19.6 GHz clock frequency," in *IoP Journals Superconductor Science and Technology*, pp. 1065 – 1070, Nov. 2001.

[24] URL: http://www.rfel.com/download/D04026_FFT_Product_Sheet.pdf